

Non-isothermal kinetics of the thermal decomposition of sodium oxalate $\text{Na}_2\text{C}_2\text{O}_4$

Nopsiri Chaiyo · Rangson Muanghlua ·
Surasak Niemcharoen · Banjong Boonchom ·
Panpailin Seeharaj · Naratip Vittayakorn

Received: 22 March 2011 / Accepted: 17 May 2011 / Published online: 3 June 2011
© Akadémiai Kiadó, Budapest, Hungary 2011

Abstract The thermal transformation of $\text{Na}_2\text{C}_2\text{O}_4$ was studied in N_2 atmosphere using thermo gravimetric (TG) analysis and differential thermal analysis (DTA). $\text{Na}_2\text{C}_2\text{O}_4$ and its decomposed product were characterized using a scanning electron microscope (SEM) and the X-ray diffraction technique (XRD). The non-isothermal kinetic of the decomposition was studied by the mean of Ozawa and Kissinger–Akahira–Sunose (KAS) methods. The activation energies (E_a) of $\text{Na}_2\text{C}_2\text{O}_4$ decomposition were found to be consistent. Decreasing E_a at increased decomposition temperature indicated the multi-step nature of the process.

Electronic supplementary material The online version of this article (doi:10.1007/s10973-011-1675-6) contains supplementary material, which is available to authorized users.

N. Chaiyo · N. Vittayakorn
Electroceramic Research Laboratory, Department of Chemistry,
Faculty of Science, College of Nanotechnology, King Mongkut's
Institute of Technology Ladkrabang, Bangkok 10520, Thailand

N. Chaiyo · N. Vittayakorn
ThEP Center, CHE, 328 Si Ayutthaya Rd, Bangkok 10400,
Thailand

R. Muanghlua · S. Niemcharoen
Department of Electronics, Faculty of Engineering, King
Mongkut's Institute of Technology Ladkrabang, Bangkok
10520, Thailand

B. Boonchom (✉)
King Mongkut's Institute of Technology Ladkrabang,
Chumphon Campus, 17/1 M. 6 Pha Thiew District, Chumphon,
86160, Thailand
e-mail: kbbanjon@gmail.com

P. Seeharaj · N. Vittayakorn (✉)
Department of Chemistry, Faculty of Science, King Mongkut's
Institute of Technology Ladkrabang, Bangkok 10520, Thailand
e-mail: naratipcmu@yahoo.com

The possible conversion function estimated through the Liqing–Donghua method was 'cylindrical symmetry (R_2 or $F_{1/2}$)' of the phase boundary mechanism. Thermodynamic functions (ΔH^* , ΔG^* and ΔS^*), calculated by the Activated complex theory and kinetic parameters, indicated that the decomposition step is a high energy pathway and revealed a very hard mechanism.

Keywords Sodium oxalate · Decomposition · Ozawa method · Kissinger–Akahira–Sunose method

Introduction

Thermal analysis (TA), e.g., thermogravimetry (TG), differential thermal analysis (DTA), and differential scanning calorimetry (DSC) have been used widely for scientific and practical purposes [1, 2]. These techniques provide important information about physico-chemical parameters, kinetic analysis, polymorphic forms, stability of material, etc., which are reliable and necessary [3]. Thus, the outcomes obtained through this basis can be applied directly in material science for studying thermal behavior, thermal character, and the mechanism and kinetic of solid state reaction. The interpretation of data obtained from these methods, use of various mathematical models and calculation procedures are quite useful. For gaining value of the apparent activation energy, E_a , and pre-exponential factor, A , which is the most probable mechanism function $g(\alpha)$ of the reaction, various equations and methods were described such as the Coats and Redfern equation [4], and iterative procedure, i.e., the Ozawa equation [5], Kissinger–Akahira–Sunose (KAS) equation [6], Senum and Yang approximation formulae [7], etc. The mathematical apparatus and calculation procedures used are related to the mathematical

analysis of thermogravimetric curves. The calculations, based on multiple rates of thermogravimetric curves, are so-called iso-conversional calculation procedures [3].

Thermal decomposition of metal oxalates has been the subject of many researches for more than a century [8]. Decomposition and its non-isothermal kinetics, belonging to some of the oxalates ($\text{Ag}_2\text{C}_2\text{O}_4$, NiC_2O_4 , MnC_2O_4 , HgC_2O_4 , PbC_2O_4 , and $\text{SrTiO}(\text{C}_2\text{O}_4)_2 \cdot 4\text{H}_2\text{O}$), were reported later [3, 8–10]. The dehydration kinetics of $\text{CaC}_2\text{O}_4 \cdot \text{H}_2\text{O}$ were deduced from the multiple rate iso-temperature method, and the apparent activation energy, E_a , was obtained from the Ozawa and KAS method [6]. The kinetic triplet, the activation energy, E_a , the pre-exponential factor, A , and the mechanism functions, $f(\alpha)$, of $\text{MgC}_2\text{O}_4 \cdot 2\text{H}_2\text{O}$ were obtained by analyzing the TG-DTG curves of their thermal decomposition using the Popescu and Flynn–Wall–Ozawa method [11]. Furthermore, the decomposed products, e.g., oxide or metal, which possess pores, lattice imperfections and both characteristics, were determined, and the results are necessary data for their function and further study. Although there has been increasing interest in the study of experimental factors and processing parameters, especially in determining the kinetics of thermal decomposition reactions, many features of oxalate decomposition still remain unclear.

In a previous paper, we presented results on the preparation of lead-free piezoelectric sodium niobate (NaNbO_3) powders [12]. The use of $\text{Na}_2\text{C}_2\text{O}_4$ as starting material (instead of Na_2CO_3) resulted in a low-temperature solid-state reaction. In general, the sodium oxalate, $\text{Na}_2\text{C}_2\text{O}_4$, serves as a metal cleaning preparation in the textile, leather and tanning industries; potassium oxalate cleans natural fibers in photography, and both of them are used in analytical and solvent extraction chemistry (sodium oxalate as primary volumetric standard for manganometry and acidimetry) [13]. As starting material for versatile industries, it is very important to determine its thermal decomposition mechanism, kinetics and thermodynamic parameter for advantages in cost and time management for industrial production. Many works on the isothermal kinetic of thermal decomposition of oxalate compounds have been published, but there are no reports on the thermal decomposition kinetic of $\text{Na}_2\text{C}_2\text{O}_4$ in the literature.

In this work, the thermal decomposition of $\text{Na}_2\text{C}_2\text{O}_4$ was investigated using non-isothermal thermogravimetry–differential thermal analysis (TG-DTG/DTA), X-ray powder diffraction (XRD), and scanning electron microscopy (SEM). Thus, the non-isothermal kinetics analysis for the decomposition of this compound was carried out, based on the iso-conversional techniques of the Ozawa and Kissinger–Akahira–Sunose (KAS) methods. Possible conversion functions have been estimated by the Liqing–Donghua method [6], combined with 35 algebraic expressions of the

conversion functions, $g(\alpha)$. The activation energy, E , and pre-exponential factor, A , were estimated. The transition state thermodynamic functions, ΔH^* , ΔG^* and ΔS^* , were calculated via the activated complex theory.

Experimental procedure

Materials and measurement

Sodium oxalate, $\text{Na}_2\text{C}_2\text{O}_4$ ($\geq 99.0\%$ (RT) 71801, Fluka), was used without further purification. Thermal behavior of $\text{Na}_2\text{C}_2\text{O}_4$ was investigated using TG-DTA (Perkin Elmer). Initial experiments were conducted with a heating rate of 15, 20, 30 and 40 K min^{-1} in a temperature range from room temperature to 1,573 K in N_2 atmosphere at a rate of $100 \text{ cm}^3 \text{ min}^{-1}$. Then, decomposition of the sample was carried out at 873 K in a furnace for 4 h using a heating/cooling rate of 10 K min^{-1} . $\text{Na}_2\text{C}_2\text{O}_4$ and its thermal transformation products were investigated further. The phase formation was studied by room temperature X-ray diffraction (XRD, Advance D8), using Ni-filtered CuK_α radiation. Sample scanning was done between the angles of $20\text{--}80^\circ$. Diffraction peaks were analyzed and indexed according to the diffracting planes of different phases. The morphology of samples was examined using a scanning electron microscope (SEM, Hitachi S4700) after gold coating.

Determination of the most probable mechanism function

Since the kinetic parameters depend strongly on the selection of a proper mechanism function for the process, the following equation was used to estimate the most correct reaction mechanism, i.e., $g(\alpha)$ function [6]:

$$\ln g(\alpha) = \left[\ln \frac{AE}{R} + \ln \frac{e^{-x}}{x^2} + \ln h(x) \right] - \ln \beta \quad (1)$$

where A (the pre-exponential factor/ min^{-1}) and E_x (the activation energy/ kJ mol^{-1}) are the Arrhenius parameters, and R is the gas constant ($8.314 \text{ J mol}^{-1} \text{ K}^{-1}$). For determination, the degrees of conversion α (extent of conversion, $\alpha = (m_i - m_t)/(m_i - m_f)$, where m_i , m_f , and m_t are the initial, final, and current sample mass, respectively, at moment t), corresponding to four heating rates ($\beta = 15, 20, 30$ and 40 K min^{-1}) taken at the same temperature, were substituted into the left side of Eq. 1, which was combined with 35 types of mechanism functions [14–16]. Plotting $\ln g(\alpha)$ versus $\ln \beta$ and a linear regression of least square method were conducted. The most probable mechanism function was assumed to be the one for which the

slope of the straight line was closest to -1.0000 , and the linear correlation coefficient r^2 should be unity.

Calculation of activation energy by iso-conversional procedure

In the kinetic study, the first Ozawa equation [5] was used to calculate the values of the activation energy, E_α , of the decomposition reaction of $\text{Na}_2\text{C}_2\text{O}_4$, as follows:

$$\ln \beta = \ln \frac{0.0048AE}{g(\alpha)R} - 1.0516 \frac{E}{RT} \tag{2}$$

and Kissinger–Akahira–Sunose (KAS) equation [6]:

$$\ln \frac{\beta}{T^2} = \ln \frac{AE}{g(\alpha)R} - \frac{E}{RT} \tag{3}$$

The kinetics of such reactions is described by various equations, taking into account the special features of their mechanisms. Data from four TG curves in the decomposition range were used to determine α from experiments at different heating rates ($\beta = 15, 20, 30$ and 40 K min^{-1}). The plots of $\ln \beta$ versus $1/T$ (Eq. 2) and $\ln (\beta/T^2)$ versus $1/T$ (Eq. 3) have provided evidence of apparent activation energy values for decomposition at different values of α . The activation energy, E_α , can be estimated from the slope of these plots. This is a model-free method according to the reaction mechanism, and the shape of $g(\alpha)$ function cannot affect this calculation, which was performed without use of the most probable mechanism function.

Calculation of the transition state thermodynamic function

The pre-exponential factor, A , can be estimated from the intercept of the plots from Ozawa (Eq. 2) and KAS (Eq. 3) through the insertion of the most probable function, $g(\alpha)$, and the calculated activation energy, E_α . According to the theory of the activated complex (transition state) of Eyring [2, 3, 17], the general equation of A may be written as follows:

$$A = \frac{e\chi k_B T_P}{h} \exp\left(\frac{\Delta S^*}{R}\right) \tag{4}$$

where $e = 2.7183$ is the Neper number; χ is the transition factor, which is unity for monomolecular reactions; k_B is the Boltzmann constant; h is Plank’s constant; and T_P is the average temperature of the TG curves at different heating rates. Then, the change of entropy may be calculated according to the formula:

$$\Delta S^* = R \ln \frac{Ah}{e\chi k_B T_P} \tag{5}$$

Therefore, the changes of the enthalpy, ΔH^* , and Gibbs free energy, ΔG^* , for the activated complex formation

from the reagent can be calculated using the well-known thermodynamical equation:

$$\Delta H^* = E - RT_P \tag{6}$$

$$\Delta G^* = \Delta H^* - T_P \Delta S^* \tag{7}$$

Results and discussion

Thermogravimetry–differential thermal analysis curves of the thermal decomposition of $\text{Na}_2\text{C}_2\text{O}_4$ at a heating rate of 30 K min^{-1} are illustrated in Fig. 1. The TG curve accordingly revealed a weight loss of $\sim 21\%$, which occurred during the temperature rise from 800 to 870 K. This observation corresponded to the endothermic peak of the DTA and DTG curve, which centred at 848 and 844 K, respectively. This decomposition step may be related to the decomposition of $\text{Na}_2\text{C}_2\text{O}_4$ to Na_2CO_3 and released CO because the overall weight loss of $\sim 21\%$ is close to the theoretical value of 20.9%, which corresponds to the release of 1 mol of CO. The decomposition reaction is suggested to be as the Eq. 8:



This decomposition temperature of the decarbonylation stage was higher than those found in the literature, which lie on the temperature of 773 K [18].

The XRD patterns of sodium oxalate ($\text{Na}_2\text{C}_2\text{O}_4$) powder and its calcined product (at 873 K) are illustrated in Fig. 2. The diffraction pattern of $\text{Na}_2\text{C}_2\text{O}_4$ powder could correspond to the monoclinic sodium oxalate (JCPDS file no. 49-1816 (▼), space group $P2_1/a$ (14)). After calcination at 873 K for 4 h, the diffraction pattern suggests an appearance of the monoclinic, γ - Na_2CO_3 [JCPDS no. 72-0628,

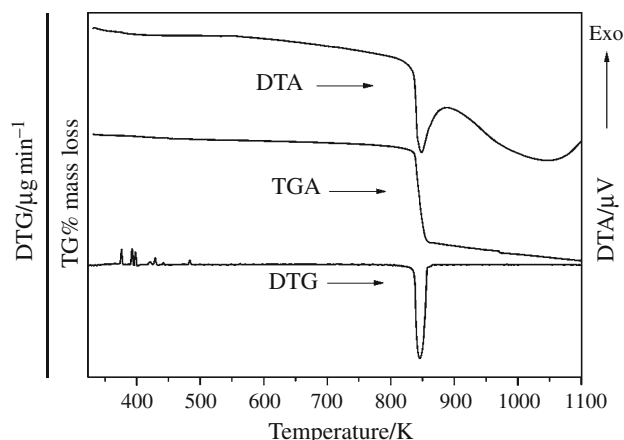


Fig. 1 TGA, DTG, and DTA curves of the thermal decomposition of $\text{Na}_2\text{C}_2\text{O}_4$ at a heating rate β of 30 K min^{-1}

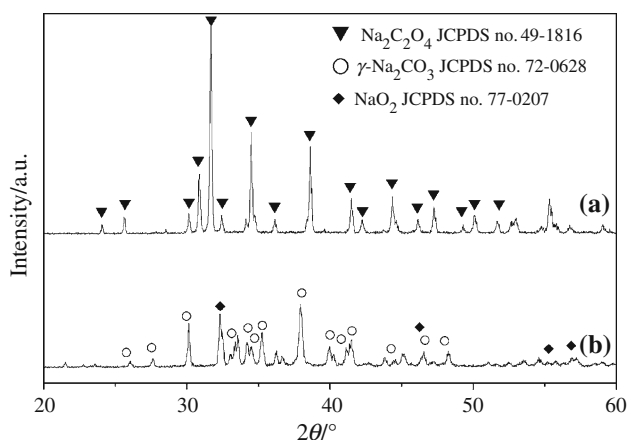


Fig. 2 X-ray diffraction patterns of *a* $\text{Na}_2\text{C}_2\text{O}_4$ and *b* its calcined product heated at 873 K for 4 h with a heating/cooling rate of 10 K min^{-1}

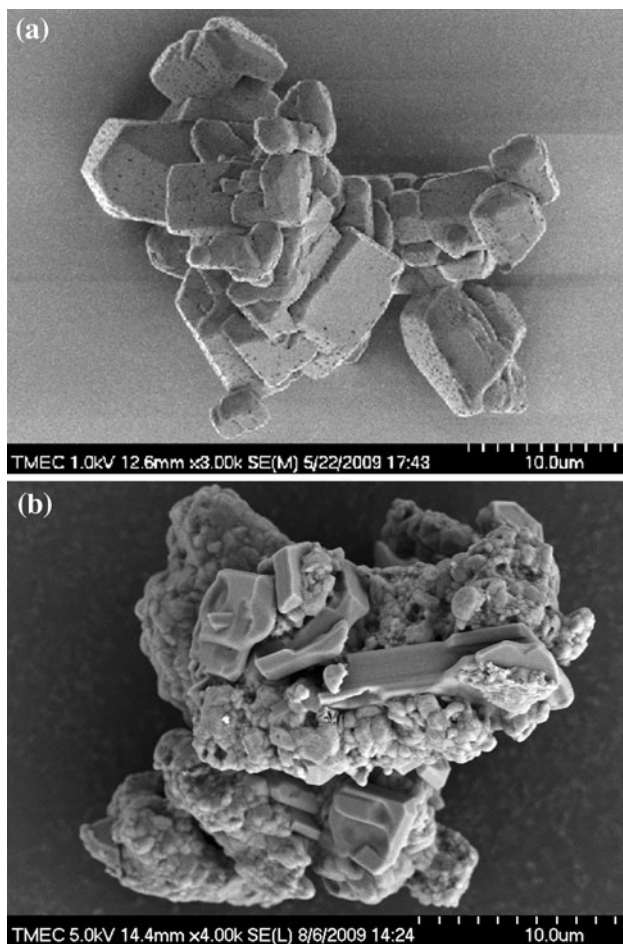


Fig. 3 SEM micrographs of $\text{Na}_2\text{C}_2\text{O}_4$ powder (*a*) and its calcined product heated at 873 K for 4 h with a heating/cooling rate of 10 K min^{-1} (*b*)

space group C2/m (12)], accompanied by the cubic NaO_2 (JCPDS file no. 77-0207, space group $\text{Fm}\bar{3}\text{m}$) as a minority phase. This result could be correlated to TGA-DTG/DTA

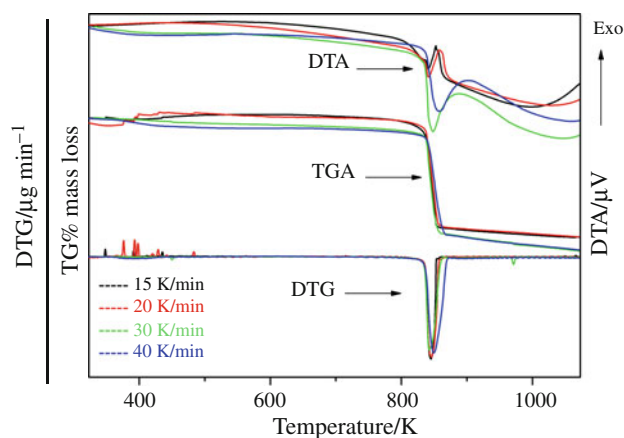


Fig. 4 TGA curves of thermal $\text{Na}_2\text{C}_2\text{O}_4$ decomposition at four heating rates under an N_2 atmosphere

Table 1 The α - T data at different heating rates for the decomposition process of $\text{Na}_2\text{C}_2\text{O}_4$

α	Temperature at four heating rate ($\beta/\text{K min}^{-1}$)				T_p/K
	15	20	30	40	
0.1	837.14	838.99	840.93	842.40	839.86
0.2	839.43	841.15	843.65	845.23	842.36
0.3	840.95	842.23	844.85	846.54	843.64
0.4	843.16	844.70	847.15	849.14	846.04
0.5	844.38	846.00	849.35	851.64	847.84
0.6	846.72	848.48	851.15	852.94	849.82
0.7	848.77	850.68	853.65	855.54	852.16
0.8	849.70	851.67	855.65	858.19	853.80
0.9	851.92	854.35	858.15	860.95	856.34

T_p is the average temperature peak in the DTG curve (K)

analysis, which suggested that the decomposition of $\text{Na}_2\text{C}_2\text{O}_4$ to Na_2CO_3 was in the region of this temperature.

The scanning electron micrographs of $\text{Na}_2\text{C}_2\text{O}_4$ powder and its calcined product (at 873 K) are illustrated in Fig. 3a, b, respectively. $\text{Na}_2\text{C}_2\text{O}_4$ powder was found to have uniform morphological features, with a polyhedral shape and obvious edges. The particle was in the range of micron size. On the contrary, the micrograph of the particle's calcined product (at 873 K) consisted of non-uniform grain. The macropores and agglomeration, which could result from the thermal decomposition process, were found.

Figure 4 shows the TG, DTG, and DTA curves in the decomposition range of $\text{Na}_2\text{C}_2\text{O}_4$, with four heating rates of 15, 20, 30, and 40 K min^{-1} . Data of α and T collected from the TG curves in the decomposition range of $0.1 < \alpha < 0.9$ at various heating rates are illustrated in Table 1, and used to determine the kinetic parameters of the process in all calculation procedures. According to Eq. 3 combined with 35 conversion functions, $\ln g(\alpha)$

calculated different α values at the same temperature, and four heating rates on $\ln \beta$, must give rise to straight lines, so the slope and linear correlation coefficient, r^2 , can be determined. Table 2 lists the results for all of the 35 types of mechanism functions. The slope determined from function no. 18 was found to be the closest to -1.0000 and the correlation coefficient, r^2 , was better than others. This function was considered to be the most probable reaction mechanism for the description of $\text{Na}_2\text{C}_2\text{O}_4$ decarboxylation. Therefore, it can be stated that the mechanism function for the decomposition of $\text{Na}_2\text{C}_2\text{O}_4$ (splitting of carbon

monoxide) is the mechanism of phase boundary reaction (cylindrical symmetry, R_2 or $F_{1/2}$ model) with integral form $g(\alpha) = 1 - (1 - \alpha)^{1/2}$ and differential form $f(\alpha) = 2(1 - \alpha)^{1/2}$.

Figure 5a, b illustrate the plots of $\ln \beta$ versus $1/T$ (Eq. 1) and $\ln(\beta/T^2)$ versus $1/T$ (Eq. 2) for the decomposition process of $\text{Na}_2\text{C}_2\text{O}_4$, based on the Ozawa and KAS analysis, respectively. The activation energy, E_x , of the decomposition reaction of $\text{Na}_2\text{C}_2\text{O}_4$, which was calculated from the slope of these straight lines and their correlation coefficient, r^2 , are tabulated in Table 3a (Ozawa method) and b (KAS method). The calculated activation energies obtained from different equations, in which the values obtained by the KAS method were generally higher, were found to be consistent. It can be seen that the values of E_x tend to decrease with the increase of conversion α . It can be noted also that the E_x values are dependent on α , and the decomposition reaction should be interpreted in terms of a multi-step reaction mechanism [19]. As the dependence can disclose the complexity of a process and identify its kinetic scheme, the shape of the decreasing dependence of E_x on α has been identified from model data [20]. This

Table 2 The most probable mechanism function, $g(\alpha)$, slope and correlation coefficient of the linear regression, r^2

No.	Symbol	Slope	r^2
1	$F_{1/3}$	-0.9571	0.984568
2	$F_{3/4}$	-1.1987	0.980565
3	$F_{3/2}$	-1.5708	0.964395
4	F_2	-1.8641	0.956190
5	F_3	-2.5481	0.946691
6	$P_{3/2}$	-1.2699	0.980378
7	$P_{1/2}$	-0.4233	0.980378
8	$P_{1/3}$	-0.2822	0.980378
9	$P_{1/4}$	-0.2116	0.980378
10	E_1	-	-
11	A_1, F_1	-1.3266	0.974513
12	$A_{3/2}$	-0.8844	0.974513
13	A_2	-0.6633	0.974513
14	A_3	-0.4422	0.974513
15	A_4	-0.3317	0.974513
16	A_u	-	-
17	R_1, F_0, P_1	-0.8466	0.980378
18	$R_2, F_{1/2}$	-1.0327	0.985949
19	$R_3, F_{2/3}$	-1.1326	0.984293
20	D_1	-1.6932	0.980378
21	D_2	-2.1589	0.986125
22	D_3	-2.26526	0.984293
23	D_4	-1.9923	0.984810
24	D_5	-2.9668	0.967651
25	D_6	-1.5714	0.980464
26	D_7	-1.6103	0.980442
27	D_8	-1.4596	0.980466
28	G_1	-0.6622	0.969938
29	G_2	-0.5652	0.961585
30	G_3	-0.5016	0.955476
31	G_4	-2.6533	0.974513
32	G_5	-3.9799	0.974513
33	G_6	-5.3069	0.974513
34	G_7	-0.5163	0.985949
35	G_8	-0.5663	0.984293

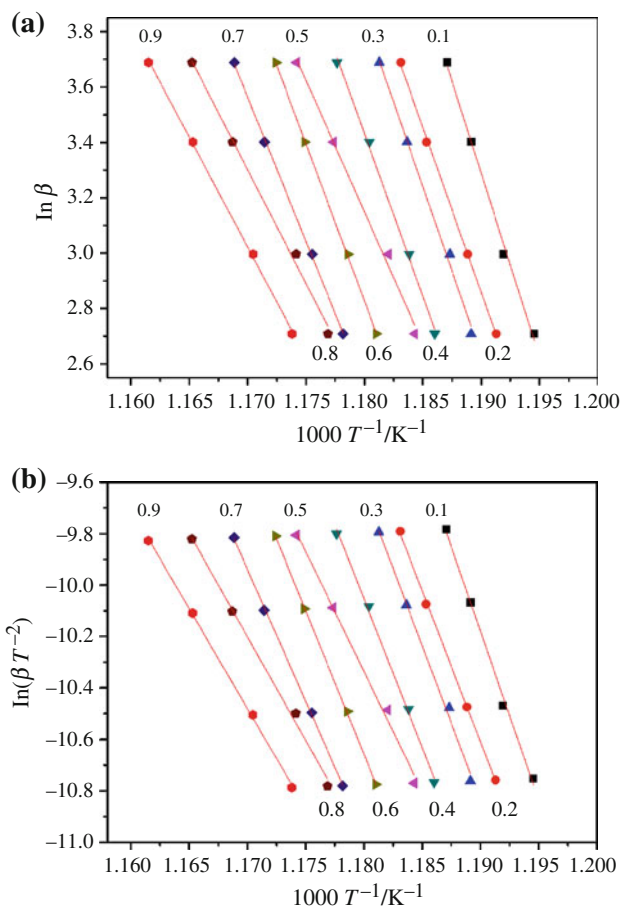


Fig. 5 Ozawa (a) and KAS (b) plots for the decomposition process of $\text{Na}_2\text{C}_2\text{O}_4$ at four heating rates in various conversions ($\alpha = 0.1-0.9$, with 0.1 increment)

Table 3 Kinetic (E_a , A), and thermodynamic (ΔS^* , ΔH^* and ΔG^*) parameters for the decarboxylation of $\text{Na}_2\text{C}_2\text{O}_4$ obtained by the Ozawa (a) and KAS (b) methods

α	$E_a/\text{kJ mol}^{-1}$	A/min^{-1}	$\Delta H^*/\text{kJ mol}^{-1}$	$\Delta S^*/\text{J mol}^{-1} \text{K}^{-1}$	$\Delta G^*/\text{kJ mol}^{-1}$	r^2
(a) Ozawa method						
0.1	1051.98	1.3231E+66	1044.9943	1003.9768	201.7900	0.9959
0.2	942.49	1.3766E+59	935.4897	870.2758	202.4000	0.9995
0.3	964.60	4.6238E+60	957.5909	899.4801	198.7519	0.9959
0.4	927.96	1.8404E+58	920.9318	853.5098	198.8303	0.9979
0.5	751.04	7.5773E+46	743.9932	635.5338	205.1614	0.9950
0.6	895.87	1.4111E+56	888.8045	812.9774	197.9180	0.9998
0.7	824.27	3.1738E+51	817.1834	723.9749	200.2424	0.9995
0.8	650.67	2.6314E+40	643.5705	511.8200	206.5770	0.9962
0.9	627.76	8.6070E+38	620.6462	483.3606	206.7244	0.9994
AV.	848.52 \pm 145.87	1.4701E+65	841.4672	754.9899	202.0440	0.9977
(b) KAS method						
0.1	1092.30	1.17385E+57	1085.3129	830.6884	387.6474	0.9958
0.2	977.12	1.21573E+50	970.1163	696.9493	383.0307	0.9994
0.3	1000.35	4.06853E+51	993.3349	726.1232	380.7471	0.9957
0.4	961.78	1.61107E+49	954.7451	680.1103	379.3461	0.9978
0.5	775.70	6.62753E+37	768.6466	462.1270	376.8362	0.9949
0.6	927.96	1.22539E+47	920.9005	639.5107	377.4298	0.9998
0.7	852.63	2.74479E+42	845.5462	550.4743	376.4552	0.9995
0.8	670.04	2.27637E+31	662.9459	338.3219	374.0857	0.9960
0.9	645.92	7.40872E+29	638.7983	309.8210	373.4858	0.9994
AV.	878.20 \pm 153.48	1.30428E+56	871.1496	581.5696	378.7849	0.9976

study reported that the decomposition reaction was complicated by diffusion. This process is met widely in solids decomposed in the following way: solid \rightarrow solid + gas [21]. In addition, values of the correlation coefficient, r^2 , for all cases of calculation were greater than 0.9949. It can be seen that the values of E_a obtained from the Ozawa and KAS methods (Eqs. 2, 3) are reliable.

On the basis of TG curves at four heating rates and using Eqs. 1–3, values of the apparent activation energy, E_a , were calculated, and the most probable reaction mechanism function of the studied reaction was determined. Based on these results, the pre-exponential factor, A , can be estimated from intercept of the plots from the Ozawa (Eq. 2) and KAS (Eq. 3) methods. The related transition state thermodynamic functions (ΔS^* , ΔH^* and ΔG^*) also can be calculated according to Eqs. 5–7. The corresponding values are shown in Table 3a (Ozawa method) and b (KAS method). As seen from Table 3a (Ozawa method) and b (KAS method), the change of the entropy, ΔS^* , for the decomposition of $\text{Na}_2\text{C}_2\text{O}_4$ is positive and can be described as corresponding activated complexes that have a lower degree of arrangement (higher entropy) than the initial state. Regarding the fundamentals of the activated complex theory (transition theory) [2, 3, 13, 14], a positive

value of ΔS^* indicates a malleable activated complex that leads to very many degrees of rotation and vibration freedom, which results in a “fast” stage reaction. On the other hand, a negative value of ΔS^* suggests that the degree of structural complexity (arrangement, organization) of the activated complex is higher than that in the non activated complex, and may be indicated as “slow” stage [19, 22–25]. The positive value of the activation enthalpy, ΔH^* , showed that the decomposition stage is connected to the introduction of heat, and agrees well with the endothermic peak in the DTA result. The high ΔH^* value indicated that this decomposition step needs high energy. The positive value of Gibbs energy, ΔG^* , suggested that this is a non-spontaneous process. These results indicated that the decomposition step of $\text{Na}_2\text{C}_2\text{O}_4$ is a high energy pathway and revealed a very hard mechanism.

Conclusions

In conclusion, kinetic parameters of $\text{Na}_2\text{C}_2\text{O}_4$ (decarboxylation reaction) decomposition can be determined on the basis of thermogravimetric data. The kinetics of thermal decomposition of $\text{Na}_2\text{C}_2\text{O}_4$ under non-isothermal

heating was studied using the Ozawa and KAS methods. The results obtained from these two different calculation procedures were found to correlate with each other. Values of the apparent activation energy and pre-exponential factor, and the change of entropy, enthalpy, and Gibbs free energy, the most probable mechanisms and characteristics of the process were reported. These could be the important data for further studies and synthesis of the materials involved.

Acknowledgements This work was supported by the Thailand Research Fund (TRF), Thailand Graduate Institute of Science and Technology (TGIST), and the National Nanotechnology Center (NANOTEC) NSTDA, Ministry of Science and Technology, Thailand through its “Center of Excellence Network” Program.

References

1. Wendlandt WW. Thermal methods of analysis. New York: John Wiley & Sons Inc; 1974.
2. Šesták J. Thermodynamical properties of solids. Prague: Academia; 1984.
3. Vlaev L, Nedelchev N, Gyurova K, Zagorcheva M. A comparative study of non-isothermal kinetics of decomposition of calcium oxalate monohydrate. *J Anal Appl Pyrolysis*. 2008;81:253–62.
4. Coats AW, Redfern JP. Kinetic parameters from thermogravimetric data. *Nature*. 1964;201:68–9.
5. Ozawa TA. A new method of analyzing thermogravimetric data. *Bull Chem Soc Jpn*. 1965;38:1881–6.
6. Liqing L, Donghua C. Application of iso-temperature method of multiple rate to kinetic analysis. *J Therm Anal Calorim*. 2004;78:283–93.
7. Senum GI, Yang RT. Rational approximations of the integral of the Arrhenius function. *J Therm Anal Calorim*. 1977;11:445–9.
8. L'vov BV. Kinetics and mechanism of thermal decomposition of nickel, manganese, silver, mercury and lead oxalates. *Thermochim Acta*. 2000;364:99–109.
9. Galwey AK, Brown ME. Thermal decomposition of ionic solids. Amsterdam: Elsevier; 1999.
10. Patra BS, Otta S, Bhattamisra SD. A kinetic and mechanistic study of thermal decomposition of strontium titanate oxalate. *Thermochim Acta*. 2006;441:84–8.
11. Zhang JJ, Ren N, Bai JH. Non-isothermal decomposition reaction kinetics of the magnesium oxalate dihydrate. *Chin J Chem*. 2006;24:360–4.
12. Chaiyo N, Boonchom B, Vittayakorn N. Solid-state reaction synthesis of sodium niobate (NaNbO_3) powder at low temperature. *J Mater Sci*. 2010;45:1443–7.
13. Budavari S, O'Neil M, Smith A, editors. The Merck index; An encyclopedia of chemicals, drugs and biologicals. 11th ed. Rahway: Merck Co. Inc.; 1989.
14. Šesták J, Berggren G. Study of the kinetics of the mechanism of solid-state reactions at increasing temperatures. *Thermochim Acta*. 1971;3:1–12.
15. Heide K, Höland W, Gölker H, Seyfarth K, Müller B, Sauer R. Die bestimmung kinetischer parameter endothermer zersetzungsreaktionen unter nicht-isothermen bedingungen. *Thermochim Acta*. 1975;13:365–78.
16. Zhang JJ, Ge LG, Zha XL, Dai YJ, Chen HL, Mo LP. Thermal decomposition kinetics of the Zn(II) complex with Norfloxacin in static air atmosphere. *J Therm Anal Calorim*. 1999;58:269–78.
17. Bamford CH, Tipper CFH. Comprehensive chemical kinetics. Amsterdam: Elsevier; 1980.
18. McAlexander LH, Beck CM, Burdeniuc JJ, Crabtree RH. Fluoroalkane aromatization over hot sodium oxalate. *J Fluorine Chem*. 1999;99:67–72.
19. Boonchom B, Vittayakorn N. Dehydration behavior of synthetic $\text{Al}_{0.5}\text{Fe}_{0.5}\text{PO}_4 \cdot 2.5\text{H}_2\text{O}$. *J Chem Eng Data*. 2010;55:3307–11.
20. Zhang K, Hong J, Cao G, Zhan D, Tao Y, Cong C. The kinetics of thermal dehydration of copper(II) acetate monohydrate in air. *Thermochim Acta*. 2005;437:145–9.
21. Vyazovkin S. A unified approach to kinetic processing of non-isothermal data. *Int J Chem Kinet*. 1996;28:95–101.
22. Vlaev LT, Gospodinov GG. Study on the kinetics of the isothermal decomposition of selenites from IIIB group of the periodic system. *Thermochim Acta*. 2001;370:15–9.
23. Boonchom B, Thongkam M. Kinetics and thermodynamics of the formation of $\text{MnFeP}_4\text{O}_{12}$. *J Chem Eng Data*. 2010;55:211–6.
24. Boonchom B, Kongtaweelert S. Study of kinetics and thermodynamics of the dehydration reaction of $\text{AlPO}_4 \cdot \text{H}_2\text{O}$. *J Therm Anal Calorim*. 2010;99:531–8.
25. Boonchom B, Danvirutai C, Thongkam M. Non-isothermal decomposition kinetics of synthetic serrabrancaite ($\text{MnPO}_4 \cdot \text{H}_2\text{O}$) precursor in N_2 atmosphere. *J Therm Anal Calorim*. 2010;99:357–62.